Received: 10 November 2018 | Revised: 28 January 2019 | Accepted: 28 February 2019

DOI: 10.1002/cta.2632

RESEARCH ARTICLE

WILEY

A three-leg resonant converter for two output LED lighting application with independent control

Kasi Ramakrishnareddy Ch | Shunmugam Porpandiselvi | Neti Vishwanathan

Department of Electrical Engineering, National Institute of Technology, Warangal, India

Correspondence
Kasi Ramakrishnareddy Ch, Department of Electrical Engineering, National Institute of Technology, Warangal, India.
Email: chkrkreddy_0510@student.nitw.ac.in

Summary

A three-leg resonant converter is proposed to drive two light emitting diode (LED) lamps of different power ratings. This may be required when both main and local lighting are essential. The proposed converter is operated simultaneously at two different frequencies. Two series resonant circuits are used to allow two different frequency currents. Each lamp is powered through a series resonant circuit and is controlled independently. LED lamp currents are regulated at the desired operating current by using phase-modulation control and asymmetrical duty ratio control. In addition, pulse-width modulation (PWM) dimming control is implemented for two LED lamps independently. The proposed topology has advantages of zero-voltage switching (ZVS), regulation of lamp currents, independent illumination control, and high efficiency. A 126-W prototype has been developed experimentally to confirm its working principle, performance, and validity.

KEYWORDS

DC-DC resonant converters, driver circuits, light emitting diodes

1 | INTRODUCTION

Improving the efficiency of lighting systems has become a global challenge. This is due to a significant amount of total energy being used for these systems. With the recent developments in lighting industry, light emitting diodes (LEDs) have become more popular and more accessible to general public over conventional sources. The advantages of LEDs which make them as a promising light source are high operating life, higher luminous efficiency, solid-state characteristic, eco friendliness, smooth dimming capability, low cost, and good color rendering property.[1-3] At present, LEDs have entered in almost all lighting applications like signal lighting, street lighting, indoor lighting, transportation, liquid crystal display (LCD) backlighting, architectural lighting, and parking lighting.[4-6]

The light output from LED is directly related to its forward current. For constant illumination, current needs to be regulated precisely. Therefore, LEDs are driven by constant current regulators which can be either linear or switching regulators. However, switching regulators have become a preferred driving solution for LED applications due to their

NOMENCLATURE: α_h, Phase angle in HF resonant circuit; α_l, Phase angle in LF resonant circuit; f_h, High switching frequency [Hz]; f_l, Low switching frequency [Hz]; $f_{0,1}$, High resonant frequency [Hz]; $f_{0,2}$, Low resonant frequency [Hz]; i_{d1}-i_{d4}, Switch (S_1-S_4) currents [A]; i_{Laux}, Auxiliary inductor current [A]; $i_{Laux(peak)}$, Peak current in auxiliary inductor [A]; i_{r1}, High resonant current [A]; i_{r2}, Low resonant current [A]; I_{01}, Lamp-1 output current [A]; I_{02}, Lamp-2 output current [A]; Q_1, Quality factor of HF resonant circuit; Q_2, Quality factor of LF resonant circuit; R_{ac1}, Equivalent ac resistance-1 [Ω]; R_{ac2}, Equivalent ac resistance-2 [Ω]; R_{LED1}, Resistance offered by LED lamp-1 [Ω]; R_{LED2}, Resistance offered by LED lamp-2 [Ω]; S_{dim1}, PWM dimming signal-1; S_{dim2}, PWM dimming signal-2; v_{ds1}-v_{ds4}, Drain to source voltage of S_1 to S_4 [V]; V_{DC}, Input DC voltage [V]; V_{g1}-V_{g6}, Gate to source voltage of S_1 to S_6 [V]; V_{01}, Lamp-1 output voltage [V]; V_{02}, Lamp-2 output voltage [V]

high efficiency compared with linear regulators.[7,8] As LEDs are operated from dc sources, good number of ac-dc LED driver topologies have been proposed to meet the essential objectives like power factor correction (PFC) and elimination of electrolytic capacitor to improve reliability and dimming features.[9-14] And also, DC operated driver circuits have been proposed for LED applications to enhance dc power distribution in lighting industry.[15-22] LED lighting applications need efficient light output, independent current regulation, and illumination control to reduce energy expenses. In the literature, some topologies have addressed independent current regulation and brightness control with high efficiency.[18,21,23-26]

This paper proposes a driver circuit to drive two LED lamps of different power ratings using a three-leg resonant converter. Both lamps can be controlled independently. It utilizes series resonant circuit for powering each LED lamp. Two series resonant circuits generate simultaneously two different frequency currents which are mutually unaffected. In addition, the proposed LED driver offers zero-voltage switching (ZVS), regulation of lamp currents, and pulse-width modulation (PWM) dimming. This proposed circuit is useful when both main and local lighting are needed. In commercial and domestic lighting applications, lamps of different wattages can be powered and controlled independently.

This work is structured as follows: the proposed configuration is presented in Section 2. Working principle and analysis of the proposed LED driver are explained in Section 3. In Section 4, design considerations are provided. Dimming and regulation of lamp currents are discussed in Section 5. Both simulation and experimental results are presented in Section 6. Finally, Section 7 concludes the paper.

2 | PROPOSED CONFIGURATION

The proposed three-leg resonant converter for LED applications is shown in Figure 1. Leg-1 and leg-2 form one full bridge inverter, which is operating at high frequency (HF). Similarly, leg-1 and leg-3 form another full bridge inverter. Leg-3 is switched at low frequency (LF). Series combination of L_{r1}, C_{r1}, and a full bridge rectifier formed by D_1 to D_4 is connected between leg-1 and leg-2. Similarly, series connection of L_{r2}, C_{r2}, and a full bridge rectifier formed by D_5 to D_8 is connected between leg-1 and leg-3. Inductor L_{r1} and capacitor C_{r1} are selected to respond to the fundamental component in the voltage between leg-1 and leg-2 to output stage. Inductor L_{r2} and capacitor C_{r2} respond to only LF fundamental component in the voltage between leg-1 and leg-3 to output stage. Capacitor C_{01} and C_{02} are filter capacitors which make LED lamp-1 and lamp-2 voltages constant, respectively. An auxiliary inductor L_{aux} is connected between leg-1 and leg-2 to improve ZVS conditions in switches S_1 and S_2.

3 | OPERATION AND ANALYSIS OF THE PROPOSED LED DRIVER

A. *Operation of the proposed driver*

The switches in full bridge formed by leg-1 and leg-2 are alternately switched on for 50% duty cycle and off for 50% duty cycle at fixed HF. Switches in leg-3 are alternately switched on for 50% duty cycle and off for 50% duty cycle at fixed LF. To prevent short circuit across the dc power supply, sufficient dead time must be inserted between the gate voltages of each leg. However, it is not displayed in the operating waveforms of the proposed LED driver shown in Figure 2. The switches in leg-1 and leg-2 produce a square wave voltage v_{AB}. Similarly, switches in leg-1 and leg-3 produce voltage v_{AC} which contains both HF and LF voltage waveforms. The concept of series resonance is used for powering both LED

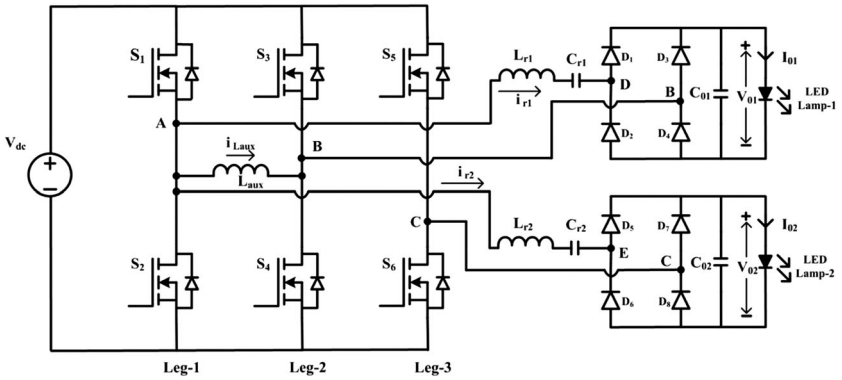

FIGURE 1 Schematic of the proposed LED driver

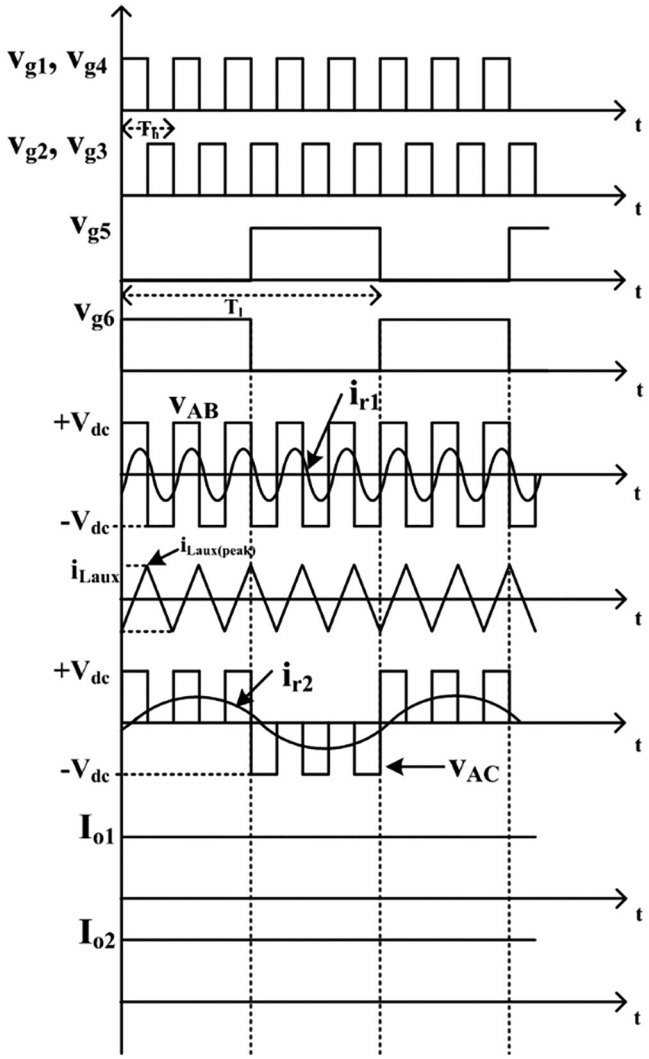

FIGURE 2 Operating waveforms of the proposed LED driver

lamps. The HF resonant circuit is formed by series connection of L_{r1} and C_{r1}, diode bridge rectifier by D_1-D_4 and LED lamp-1. The LF resonant circuit is formed by series connection of L_{r2} and C_{r2}, diode bridge rectifier by D_5 to D_8, and LED lamp-2. HF resonant circuit offers low impedance to fundamental component of v_{AB}. Thus, HF alternating current i_{r1} is generated. And it is rectified and filtered to feed LED lamp-1. Similarly, LF resonant circuit offers low impedance to only LF fundamental component of v_{AC}. Thus, LF alternating current i_{r2} is produced, which is rectified and filtered to power LED lamp-2.

B. *Analysis of the proposed LED driver*

The following assumptions are considered to analyze the proposed LED driver:

a. The converter is operating in steady state.
b. The power MOSFETs and power diodes are ideal.
c. The voltage across each LED lamp is constant.
d. The exponential decay in fundamental current during transient is neglected.

In the proposed converter, v_{AB} of magnitude V_{dc} is applied to the HF resonant circuit. Similarly, v_{AC}, which is a sum of HF and LF square waves of magnitude $V_{dc}/2$, is applied to the LF resonant circuit. These resonant circuits allow only fundamental components. Therefore, conventional AC analysis can be used to calculate the static gain of the proposed

converter. The AC equivalent circuit of the proposed LED driver circuit is shown in Figure 3A. The analysis is given for only LED lamp-1. Similar analysis is applicable to LED lamp-2.

The HF resonant circuit filters all the harmonic voltage components except the fundamental component present in the voltage v_{AB}. The AC resistance R_{ac1}, which is used in the AC equivalent circuit, accounts for the nonlinearity present in the rectifier. The reactance offered by L_{r1} and C_{r1} are denoted as X_{Lr1} and X_{Cr1} respectively. From the equivalent circuit shown in Figure 3A, the static gain of the proposed driver is represented by using a simple voltage division principle:

$$\frac{V_{DB}}{V_{AB}} = \frac{R_{ac1}}{R_{ac1} + j(X_{Lr1} - X_{Cr1})} = \frac{1}{\left[1 + j\left(\frac{X_{Lr1} - X_{Cr1}}{R_{ac1}}\right)\right]}. \tag{1}$$

Note that V_{AB} is the fundamental component of the square wave voltage applied to the HF resonant circuit and V_{DB} is the fundamental component of the square wave voltage of magnitude V_{01} across R_{ac1}. The AC resistance R_{ac1} is calculated by using the circuit shown in Figure 3B in which the resistance offered by LED lamp-1 is represented as R_{LED1}. The R_{ac1} is given by

$$R_{ac1} = \frac{V_{DB}(rms)}{I_{r1}(rms)} = \frac{4V_{01}}{\sqrt{2}\pi} \Big/ \frac{\pi I_{01}}{2\sqrt{2}} = \frac{8\,V_{01}}{\pi^2 I_{01}} = \frac{8}{\pi^2} R_{LED1} \tag{2}$$

and

$$X_{Lr1} = 2\pi f_h L_{r1} \tag{3}$$

$$X_{Cr1} = \frac{1}{2\pi f_h C_{r1}}. \tag{4}$$

The sharpness in the HF resonant current is measured by quality factor (Q_1), and it is defined by

$$Q_1 = \frac{\omega_{0,1} L_{r1}}{R_{LED1}} = \frac{1}{\omega_{0,1} C_{r1} R_{LED1}} \tag{5}$$

where, $\omega_{0,1}$ is the high resonant frequency in radians per seconds, and it is given by

$$\omega_{0,1} = 2\pi\left(f_{0,1}\right) = \frac{1}{\sqrt{L_{r1} C_{r1}}}. \tag{6}$$

Therefore, high resonant frequency in hertz is represented as

$$f_{0,1} = \frac{1}{\left[2\pi\sqrt{L_{r1} C_{r1}}\right]}. \tag{7}$$

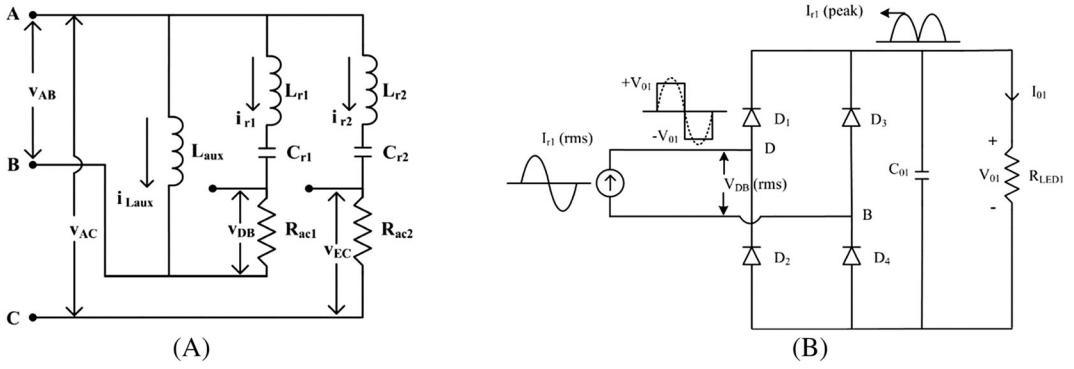

FIGURE 3 A, AC equivalent circuit. B, Equivalent circuit for R_{ac1}

By substituting Equation 2, 3, 4, and 5 in Equation 1, the gain is finally expressed as

$$\frac{V_{DB}}{V_{AB}} = \frac{{}^{4}V_{01}/_{\pi}}{{}^{4}V_{dc}/_{\pi}} = \frac{V_{01}}{V_{dc}} = \frac{1}{\left[1 + j\frac{\pi^2}{8}Q_1\left(\frac{f_h}{f_{0,1}} - \frac{f_{0,1}}{f_h}\right)\right]}. \tag{8}$$

The steady-state analysis for LED lamp-2 is similar to aforementioned analysis under 50% duty cycle of leg-3 switches. Hence, the static gain of the proposed converter with respect to LED lamp-2 is given as

$$\frac{V_{EC}}{V_{AC}} = \frac{{}^{4}V_{02}/_{\pi}}{{}^{2}V_{dc}/_{\pi}} = \frac{V_{02}}{V_{dc}} = \frac{1}{2\left[1 + j\frac{\pi^2}{8}Q_2\left(\frac{f_l}{f_{0,2}} - \frac{f_{0,2}}{f_l}\right)\right]} \tag{9}$$

where, V_{AC} is the fundamental component of the square wave voltage applied to the LF resonant circuit, V_{EC} is the fundamental component of the square wave voltage of magnitude V_{02} across R_{ac2}. Q_2 is the quality factor of the LF resonant circuit and is defined as

$$Q_2 = \frac{\omega_{0,2}L_{r2}}{R_{LED2}} = \frac{1}{\omega_{0,2}C_{r2}R_{LED2}} \tag{10}$$

and $f_{0,2}$ is the low resonant frequency in hertz and is represented as

$$f_{0,2} = \frac{1}{\left[2\pi\sqrt{L_{r2}C_{r2}}\right]}. \tag{11}$$

4 | REGULATION OF LED LAMP CURRENT AND DIMMING CONTROL

In the proposed configuration, if input voltage V_{dc} is changed, the operating voltage and current of both the LED lamps are changed. Consequently, the illumination from the both LED lamps changes. Therefore, LED lamp currents need to be regulated against variation in input dc voltage V_{dc}. To regulate LED lamp-1 current against variation in V_{dc}, phase-modulation control is used. In this control, input voltage to the HF resonant circuit v_{AB} is controlled by phase shifting the sequence of conduction for switches in leg-1 and leg-2. A phase angle (α_h) between the gate voltages of switches in leg-1 and leg-2 provides a phase-modulated voltage v_{AB} as shown in Figure 4A. Similarly, to regulate LED lamp-2 current against variation in V_{dc}, asymmetrical duty ratio control is applied for switches in leg-3. In this control, input voltage to the LF resonant circuit v_{AC} is controlled based on unequal duty cycle operation of switches in leg-3. A phase angle (α_l) between the gate voltages of switches in leg-3 achieves asymmetrical voltage v_{AC} as shown in Figure 4A. Because only fundamental voltage components are allowed by both HF and LF resonant circuit, their magnitudes[27] are given as

$$V_{AB} = \frac{4V_{dc}}{\pi}\cos\left(\frac{\alpha_h}{2}\right) \tag{12}$$

$$V_{AC} = \frac{2V_{dc}}{\pi}\cos\left(\frac{\alpha_l}{2}\right). \tag{13}$$

By substituting Equations 2, 3, 4, 5, and 12 in Equation 1, the static gain of the proposed LED driver with respect to LED lamp-1 is modified as

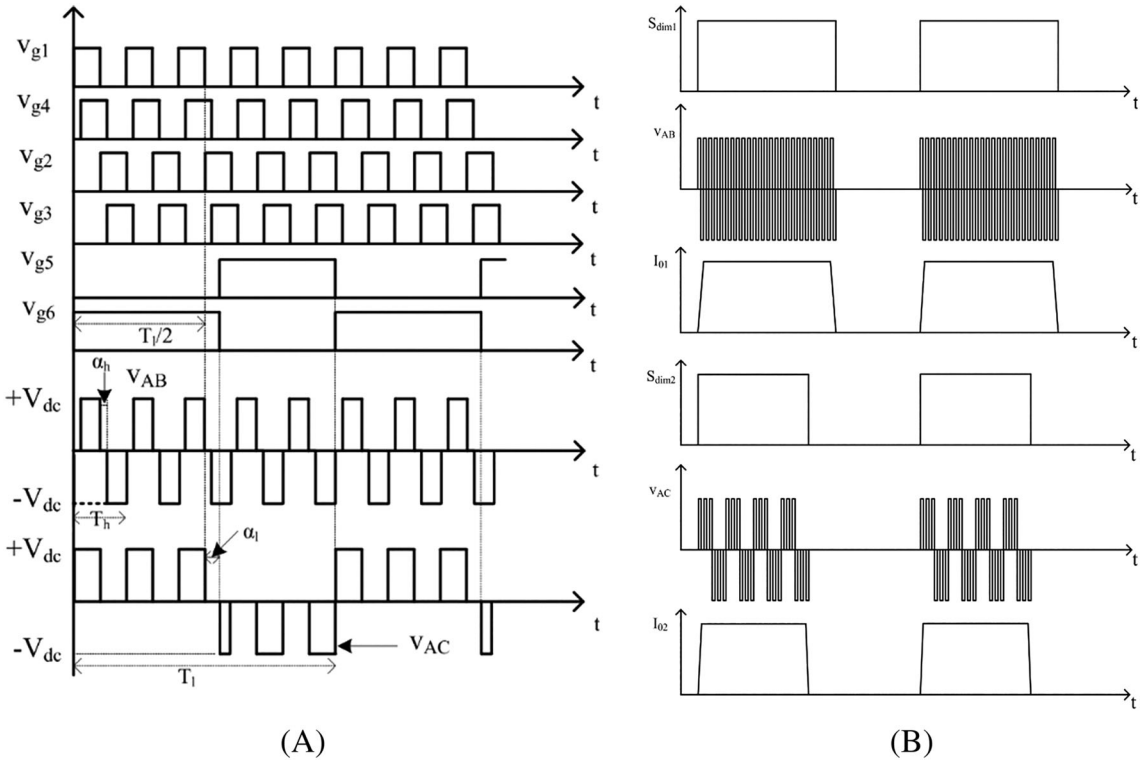

FIGURE 4 A, Switching sequence and input voltages to HF and LF resonant circuits under LED lamp regulation. B, Dimming signals and input voltages to HF and LF resonant circuits and both LED lamp currents

$$\frac{V_{01}}{V_{dc}} = \frac{\cos\left(\frac{\alpha_h}{2}\right)}{\left[1 + j\frac{\pi^2}{8}Q_1\left(\frac{f_h}{f_{0,1}} - \frac{f_{0,1}}{f_h}\right)\right]}. \tag{14}$$

By substituting Equations 2, 3, 4, 5, and 13 in Equation 1, the static gain of the proposed LED driver with respect to LED lamp-2 is modified as

$$\frac{V_{02}}{V_{dc}} = \frac{\cos\left(\frac{\alpha_l}{2}\right)}{2\left[1 + j\frac{\pi^2}{8}Q_2\left(\frac{f_l}{f_{0,2}} - \frac{f_{0,2}}{f_l}\right)\right]}. \tag{15}$$

The magnitude of input voltage V_{dc} can be found by using either Equation 14 or Equation 15 by selecting the LED lamps, high switching, and resonant frequency and low switching, and resonant frequency. The variation in V_{dc} is compensated by adjusting phase angle (α_h) in the HF resonant circuit and phase angle (α_l) in the LF resonant circuit.

Adjustable illumination in the LED lamp is called dimming. It is an important requirement for LED applications which improves power saving. Good number of techniques for dimming operation have been presented, such as amplitude modulation (AM),[28] pulse width modulation (PWM),[29] double PWM,[30] bilevel current control,[31] on-off control,[32] etc. These techniques have been employed depending upon application due to their merits and demerits. In the proposed paper, PWM dimming is incorporated independently for both LED lamps. To realize PWM dimming in LED lamp-1, the input voltage to the HF resonant circuit v_{AB} is made zero by dimming signal S_{dim1}. To implement PWM dimming in LED lamp-2, the input voltage to the LF resonant circuit v_{AC} is made zero by dimming signal S_{dim2}. Thus, average currents through both LED lamps are controlled independently without changing the operating voltage and current. The two dimming signals, voltages v_{AB} and v_{AC}, and LED lamp currents are shown in Figure 4B.

5 | DESIGN CONSIDERATIONS

The approximated model[33] of an LED is considered to select the component values of the proposed driver circuit. In the proposed LED driver, two LED lamps are used. In LED lamp-1, four parallel strings are used. In each LED string, 13 LEDs are connected in series. In LED lamp-2, four LED strings are connected in parallel. In each string, six LEDs are connected in series. The operating point for each LED is selected at 3.25 V, 510 mA. And the cut-in voltage of each LED is 2.32 V. Therefore, operating voltage and current of LED lamp-1 are 42.25 V and 2.04 A. And operating voltage and current of LED lamp-2 are 19.5 V and 2.04 A. Consequently, power consumed by LED lamp-1 and lamp-2 are 86 and 40 W, respectively.

A. *Selection of switching frequencies*

The criteria for selecting f_h and f_l should not affect the operation of HF and LF resonant circuits. The HF component of v_{AB} should power only the HF resonant circuit. The LF component of v_{AC} should power only LF resonant circuit. To make this happen, f_h should be far greater than f_l. f_h can be taken either as integer multiples or as noninteger multiples of f_l. If f_h is noninteger multiples of f_l, the effect of the harmonic component of f_l on the HF resonant circuit can be avoided to a large extent. Hence, f_h is selected at 168 kHz, and f_l is selected at 30 kHz. For ZVS, $f_{0,1}$ and $f_{0,2}$ are to be selected 5% to 10% less than f_h and f_l, respectively. Thus, $f_{0,1}$ is selected at 153 kHz, and $f_{0,2}$ is selected at 28.67 kHz.

B. *Calculation of HF resonant circuit parameters*

The product of L_{r1} and C_{r1} is obtained from Equation 7, and it is expressed as

$$L_{r1}C_{r1} = \left[\frac{1}{2\pi f_{0,1}}\right]^2. \tag{16}$$

After selecting $f_{0,1}$ as 153 kHz, Equation 16 is expressed as

$$L_{r1}C_{r1} = 1.082 \times 10^{-12}. \tag{17}$$

From Equation 5, quality factor Q_1 is expressed as

$$Q_1 = \frac{1}{R_{LED1}}\sqrt{\frac{L_{r1}}{C_{r1}}}. \tag{18}$$

With $Q_1 = 1.52$ and $R_{LED1} = 20.83\ \Omega$, from Equations 17 and 18, the inductor L_{r1} and capacitor C_{r1} are calculated as 33 μH and 33 nF, respectively. To allow a ripple current of less than 10% of I_{01} in LED lamp-1, C_{01} is selected as 1.22 μF.

C. *Calculation of LF resonant circuit parameters*

From Equation 11, the product of L_{r2} and C_{r2} is expressed as

$$L_{r2}C_{r2} = \left[\frac{1}{2\pi f_{0,2}}\right]^2. \tag{19}$$

After selecting $f_{0,2}$ as 28.67 kHz, Equation 19 is expressed as

$$L_{r2}C_{r2} = 3.082 \times 10^{-11}. \tag{20}$$

From Equation 10, quality factor Q_2 is expressed as

$$Q_2 = \frac{1}{R_{LED2}}\sqrt{\frac{L_{r2}}{C_{r2}}}. \tag{21}$$

With $Q_2 = 2.64$ and $R_{LED2} = 9.558\ \Omega$, from Equations 20 and 21, the inductor L_{r2} and capacitor C_{r2} are calculated as 140 μH and 0.22 μF, respectively. To allow a ripple current less than 10% of I_{02} in LED lamp-2, C_{02} of 14.7 μF is selected.

D. *Calculation of input dc voltage V_{dc}*

In this configuration, ±5% variation in V_{dc} is considered. The criteria to calculate V_{dc} is that at a minimum value of V_{dc}, ie (V_{dc} − 5%), the switches in all the three legs are at 50% duty ratio. In other words, voltage v_{AB} and v_{AC} are full square wave voltages. Thus, Equation 8 or Equation 9 can be used to calculate V_{dc}. With V_{01} of 42.25 V, Q_1 of 1.52, f_h of 168 kHz, and $f_{0,1}$ of 153 kHz, the input voltage V_{dc} is calculated from Equation 8 as

$$\frac{42.25}{(1-0.05)V_{dc}} = \frac{1}{\left[1 + j\frac{\pi^2}{8}1.52(0.187)\right]}.$$

$$\Rightarrow V_{dc} \cong 48V$$

After selecting V_{dc}, the phase angle α_h and α_l can be calculated from Equations 14 and 15, respectively, by substituting $V_{dc} = 48$ V.

E. *Calculation of auxiliary inductor's value L_{aux}*

TABLE 1 Parameters of the proposed LED driver

DC input voltage, V_{dc}	48 ± 5% V
High switching frequency, f_h	168 kHz
High resonant frequency, f_{r1}	153 kHz
Resonant inductor L_{r1}	33 μH
Resonant capacitor C_{r1}	0.033 μF
Output capacitor C_{01}	1.22 μF
Forward voltage of each LED	3.25 V
Operating current of each LED	510 mA
Threshold voltage of each LED	2.32 V
V_{01}	42.25 V
I_{01}	2.04 A
P_{01}	86 W
Low switching frequency, f_l	30 kHz
Low resonant frequency, f_{r2}	28.67 kHz
Resonant inductor L_{r2}	140 μH
Resonant capacitor C_{r2}	0.22 μF
Output capacitor C_{02}	14.7 μF
V_{02}	19.5 V
I_{02}	2.04 A
P_{02}	40 W
PWM dimming frequency	100 Hz
Switching devices used	IRF 540 N
Power diodes used	MUR 860
Control ICs used	UC 3875, SG 3525
Driver ICs used	IR 2110

In the proposed configuration, leg-1 is common for both HF resonant circuit and LF resonant circuit. Therefore, switches in leg-1 conduct sum of the HF resonant current (i_{r1}) and LF resonant current (i_{r2}). Hence, certain ZVS conditions are affected for leg-1. To reduce this effect, an auxiliary inductor L_{aux} is connected between leg-1 and leg-2. This inductor L_{aux} increases turn-on and off current for switches in leg-1. The voltage across L_{aux} is $\pm V_{dc}$. Hence, current through L_{aux} is triangular. And peak current through L_{aux} appears during dead time between gate voltages of leg-1 switches. The peak current through L_{aux} at V_{dc} − 5% is expressed as

$$i_{Laux(peak)} = \frac{0.95 V_{dc} T_h}{4 L_{aux}}. \tag{22}$$

The value of $i_{Laux(peak)}$is inversely proportional to the value of L_{aux} for a fixed V_{dc} and T_h. For $i_{Laux(peak)}$of 2.26 A, V_{dc} of 48 V, and T_h of 5.952 μs, L_{aux} is calculated as 30 μH.

6 | SIMULATION AND EXPERIMENTAL RESULTS

To verify the feasibility of the proposed configuration for LED applications, a total of 126-W prototype has been implemented. It is first simulated using OrCAD PSpice software, and then experimental prototype has been developed and

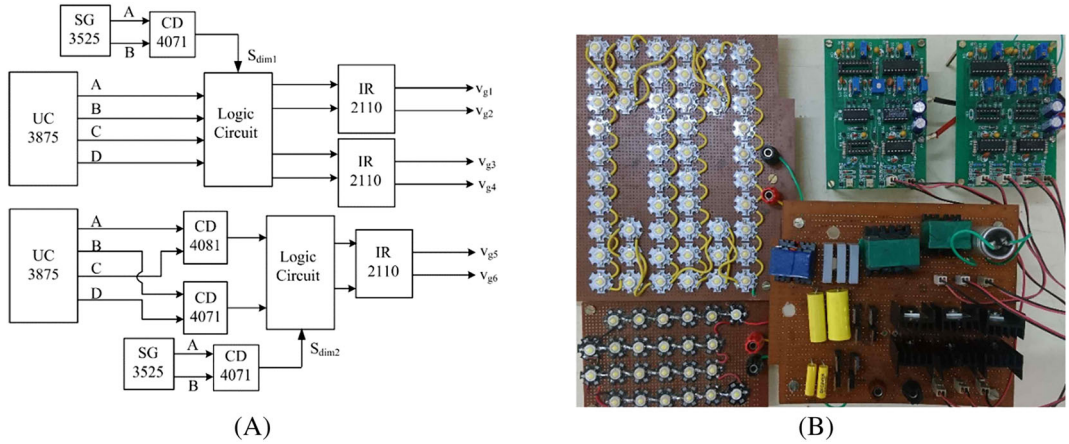

FIGURE 5 A, Schematic of control circuit of the proposed LED driver. B, Experimental prototype [Colour figure can be viewed at wileyonlinelibrary.com]

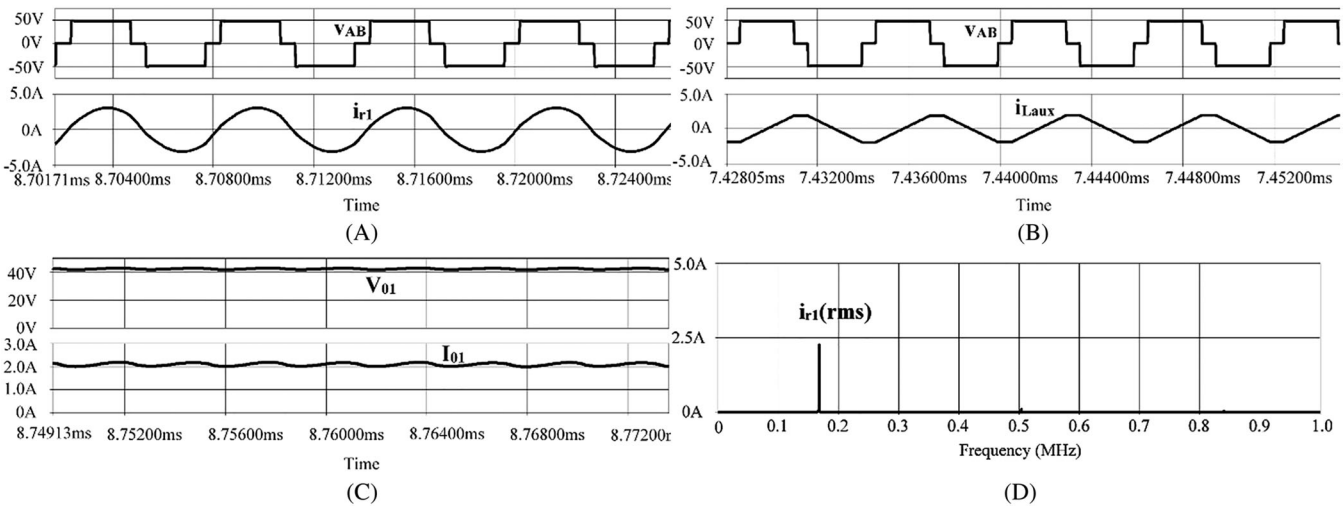

FIGURE 6 Simulated waveforms of HF resonant circuit at full illumination. A, Input voltage to the HF resonant circuit and HF resonant current. B, Input voltage to the HF resonant circuit and auxiliary inductor current. C, Voltage and current of LED lamp-1. D, FFT of HF resonant current

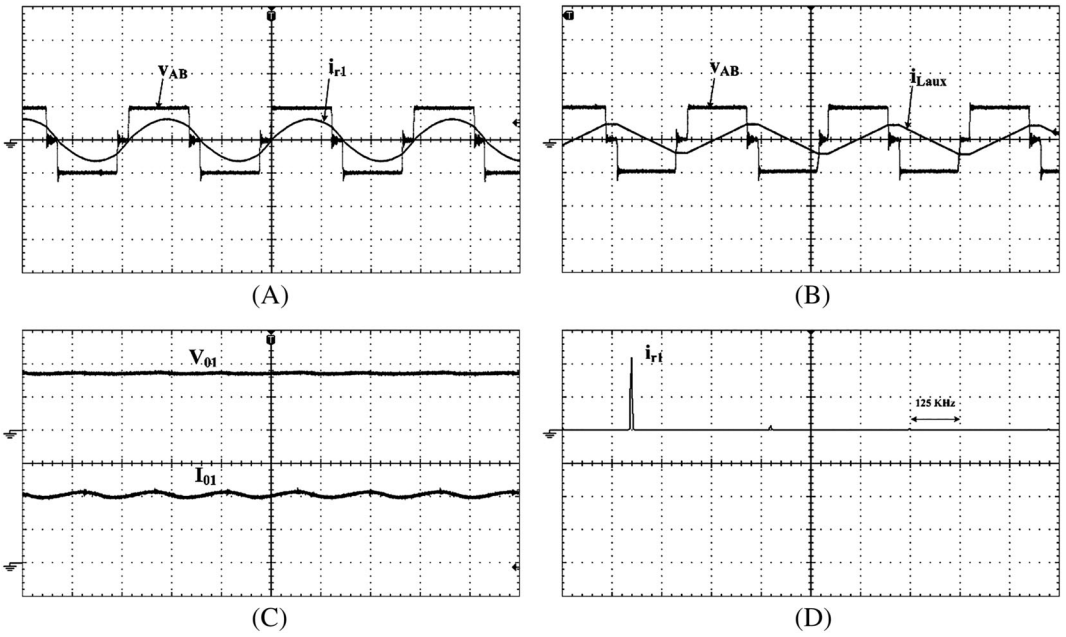

FIGURE 7 Experimental waveforms of HF resonant circuit at full illumination. A, Input voltage to the HF resonant circuit and HF resonant current (v_{AB}: 50 V/div; i_{r1}: 5 A/div; time: 2 μs/div). B, Input voltage to the HF resonant circuit and auxiliary inductor current (v_{AB}: 50 V/div; i_{Laux}: 5 A/div; time: 2 μs/div). C, Voltage and current of LED lamp-1 (V_{01}: 25 V/div; I_{01}: 1 A/div; time: 2 μs/div). D, FFT of HF resonant current (i_{r1}: 1 A/div)

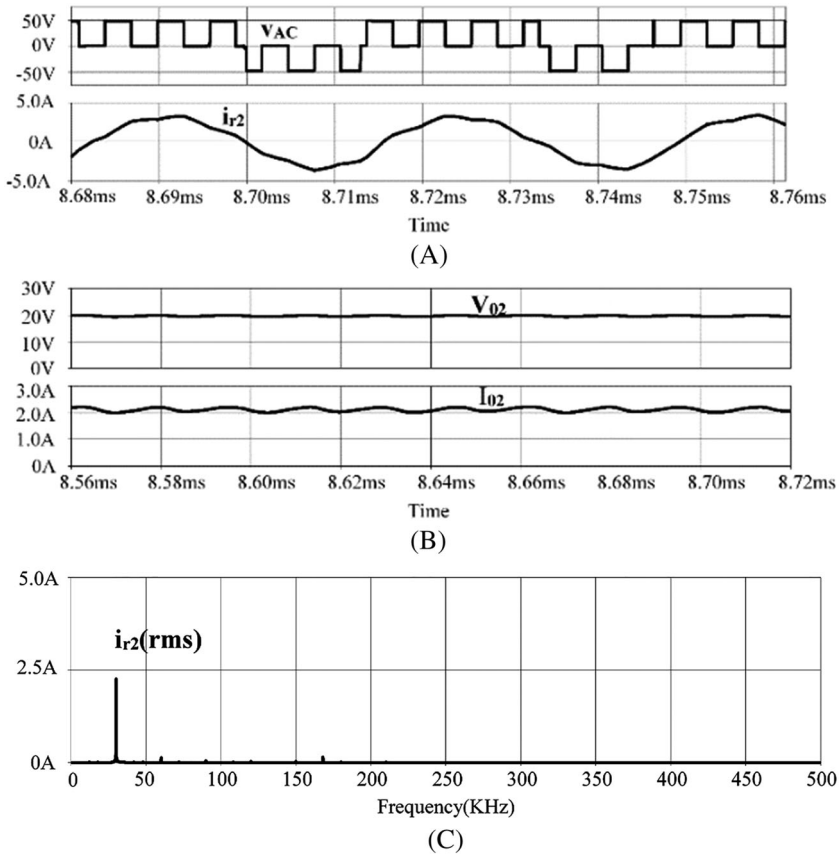

FIGURE 8 Simulated waveforms of LF resonant circuit at full illumination. A, Input voltage to the LF resonant circuit and LF resonant current. B, Voltage and current of LED lamp-1. C, FFT of LF resonant current

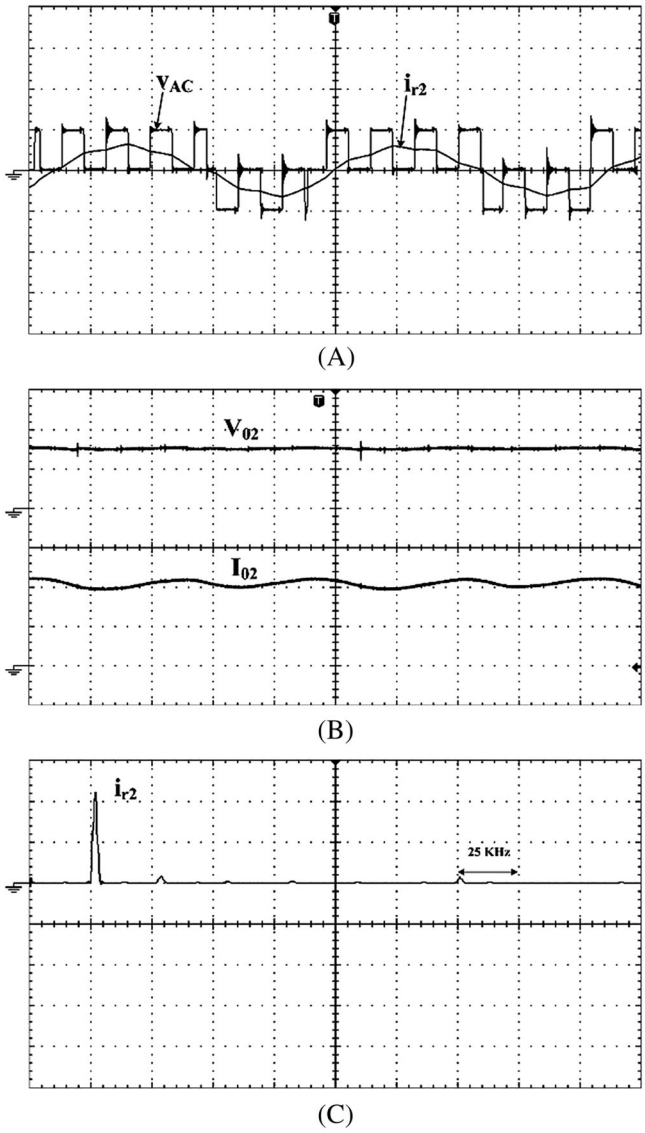

FIGURE 9 Experimental waveforms of LF resonant circuit at full illumination. A, Input voltage to the LF resonant circuit and LF resonant current (v_{AC}: 50 V/div; i_{r2}: 5 A/div; time: 8 μs/div). B, Voltage and current of LED lamp-2 (V_{02}: 12.5 V/div; I_{02}: 1 A/div; time: 8 μs/div). C, FFT of LF resonant current (i_{r2}: 1 A/div)

verified. Table 1 shows the parameters used in the proposed LED driver. Figure 5A shows the schematic of the control circuit of the proposed configuration, and the experimental prototype is shown in Figure 5B. Both LED lamps are powered with input voltage $V_{dc} = 48$ V. Figures 6 and 7 show the simulated and experimental waveforms of the proposed LED driver for the HF resonant circuit at full illumination, respectively. It is observed that the experimental waveforms of the HF resonant circuit are in good agreement with simulated waveforms. Further, fast Fourier transform (FFT) of i_{r1} shows that it has only fundamental current component and has negligible LF resonant current component. Figures 8 and 9 show the simulated and experimental waveforms of the proposed LED driver for the LF resonant circuit at full illumination, respectively.

It is observed that the experimental waveforms of the LF resonant circuit are in good agreement with simulated waveforms. Also, FFT of the LF resonant current i_{r2} shows that it has only fundamental current component and has negligible HF resonant current component. To show the ZVS feature in this LED driver, experimental switch voltage and current waveforms of HF legs are shown in Figure 10. It is observed that switches in leg-1 and leg-2 are turned on and off at zero voltage. Thus, switching losses are reduced. Hence, the efficiency of the proposed converter is high. Also, the efficiency of the proposed LED driver at full illumination level of both HF and LF resonant circuits is found to

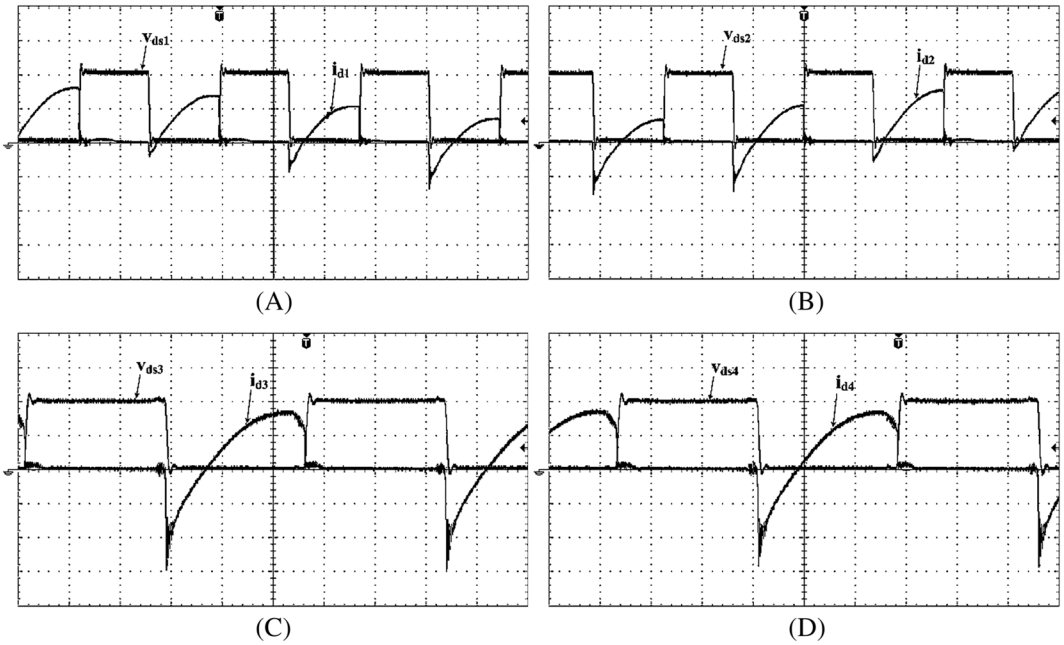

FIGURE 10 Experimental switch voltage and current waveforms at full illumination. A, Voltage and current in switch S_1 (v_{ds1}: 25 V/div; i_{d1}: 5 A/div; time: 2 μs/div). B, Voltage and current in switch S_2 (v_{ds2}: 25 V/div; i_{d2}: 5 A/div; time: 2 μs/div). C, Voltage and current in switch S_3 (v_{ds3}: 25 V/div; i_{d3}: 2 A/div; time: 1 μs/div). D, Voltage and current in switch S_4 (v_{ds4}: 25 V/div; i_{d4}: 2 A/div; time: 1 μs/div)

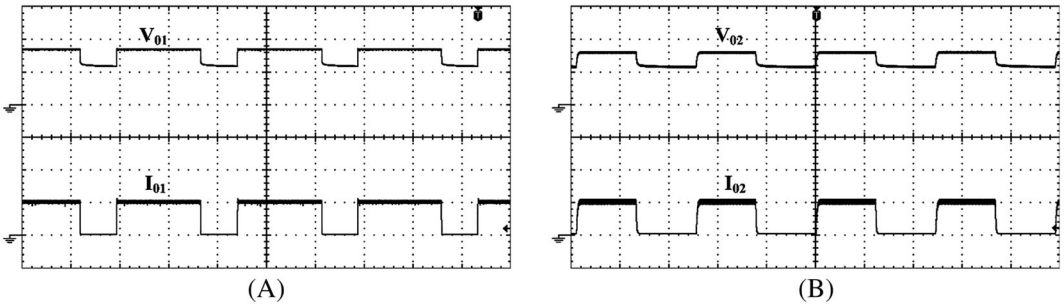

FIGURE 11 Dimming waveforms. A, Voltage and current of LED lamp-1 at 70% dimming (V_{01}: 25 V/div; I_{01}: 2 A/div; time: 4 ms/div). B, Voltage and current of LED lamp-2 at 50% dimming (V_{02}: 12.5 V/div; I_{02}: 2 A/div; time: 4 ms/div)

be 92.45%. The proposed LED driver is also powered with ±5% variation in V_{dc} at full illumination of both LED lamp-1 and lamp-2. Under −5% variation in V_{dc}, the efficiency of the driver is found to be 91.3%. And under +5% variation in V_{dc}, the efficiency of the driver is found to be 90.87%.

In the proposed LED driver, LED lamps can be dimmed independently. Figure 11A shows LED lamp-1 voltage and current at 70% of full illumination, and Figure 11B shows LED lamp-2 voltage and current at 50% of full illumination with V_{dc} = 48 V. At this illumination level, the voltage and current waveforms of switches in HF legs are shown in Figure 12. It is observed that LED lamp voltage and currents are at their operating values when their dimming signal is ON. When their dimming signal is OFF, LED lamp currents become zero, and LED lamp voltages drop below their cut-in voltages. It is also observed that switches are turned and off at zero voltage under dimming operation also. The efficiency curves of both LED lamps under various dimming levels are shown in Figure 13. Figure 13A shows the efficiency curve of LED lamp-1 under various dimming levels by keeping LED lamp-2 at full illumination. Similarly, Figure 13B shows the efficiency curve of LED lamp-2 under various dimming levels by keeping LED lamp-1 at full illumination. It is observed that high efficiency is guaranteed at any dimming level of both LED lamps. A relative comparison between the proposed topology and other topologies for LED lighting applications is given in Table 2. The proposed

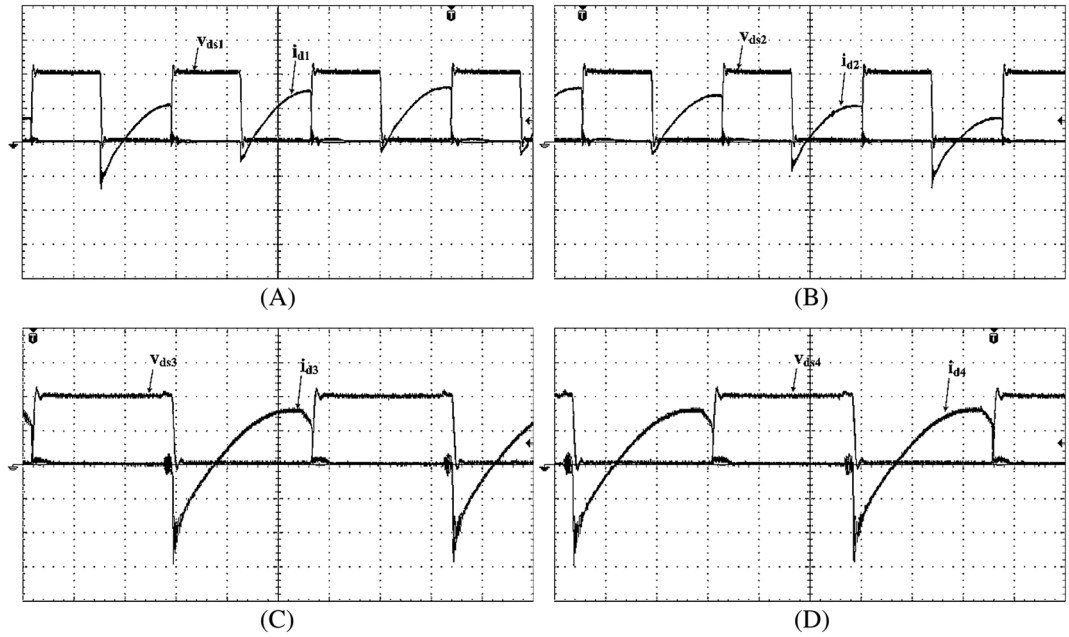

FIGURE 12 Experimental switch voltage and current waveforms under dimming operation. A, Voltage and current in switch S_1 (v_{ds1}: 25 V/div; i_{d1}: 5 A/div; time: 2 μs/div). B, Voltage and current in switch S_2 (v_{ds2}: 25 V/div; i_{d2}: 5 A/div; time: 2 μs/div). C, Voltage and current in switch S_3 (v_{ds3}: 25 V/div; i_{d3}: 2 A/div; time: 1 μs/div). D, Voltage and current in switch S_4 (v_{ds4}: 25 V/div; i_{d4}: 2 A/div; time: 1 μs/div)

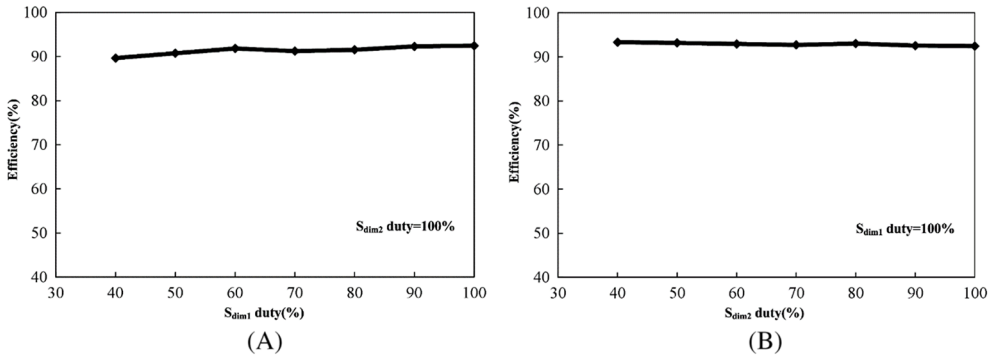

FIGURE 13 Efficiency curves of both LED lamps under various dimming levels. A, Efficiency curve of LED lamp-1 under various dimming levels. B, Efficiency curve of LED lamp-2 under various dimming levels

TABLE 2 Comparison between the proposed topology and other topologies

Feature	Ref.[18]	Ref.[21]	Ref.[23]	Ref.[24]	Ref.[25]	Ref.[26]	Proposed
ZVS	Yes	Yes	Yes	Yes	No	Yes	Yes
Input voltage	48 V DC	150 V DC	380 V DC	100-240 V AC	12 V DC	400 V DC	48 V DC
Total output power	20 W	30 W	50 W	100 W	24 W	200 W	126 W
Peak efficiency	93.4%	95.5%	90.5%	92%	91.7%	92.8%	92.45%
Component count per lamp	High	Moderate	Moderate	High	Low	High	Moderate
LED lamps	4	2	1	2	2	2	2
Wattage of all LED lamps	Different	Different	-	Same	Same	Different	Different
Dimming	Yes	Yes	Yes	Yes	No	Yes	Yes
Independent dimming	Yes	No	-	Yes	No	Yes	Yes
Extension to multiple lamps	Yes	Yes	Yes	Yes	Yes	Yes	Yes
Current regulation	Yes	No	Yes	Yes	Yes	Yes	Yes

configuration can handle large power with low input voltage. Low voltage rating switching devices and diodes can be used in this configuration. Besides, its efficiency is comparable with other configurations.

7 | CONCLUSIONS

In this paper, a three-leg converter has been developed to power two LED lamps with different power ratings. Need of lamps of different wattage may arise when both main lighting and local lighting are required. The proposed converter operates at two different frequencies simultaneously. Two series resonant circuits generate two different frequency components which are used for powering LED lamps. Both LED lamps can be regulated at the required operating voltage and current. Further, both LED lamps can be dimmed independently. Hence, this driver provides independent load control. This converter operates with ZVS. High efficiency is obtained at any dimming level of both LED lamps. The proposed topology can be suitable for smart lighting applications. It can be powered from low voltage dc grid or battery-operated systems.

ORCID

Kasi Ramakrishnareddy Ch https://orcid.org/0000-0002-0505-0408

REFERENCES

1. Bender VC, Marchesan TB, Alonso JM. Solid-state lighting: a concise review of the state of the art on LED and OLED modeling. *IEEE Ind Electron Mag*. 2015;9(2):6-16.
2. Modepalli K, Parsa L. Lighting up with a dual-purpose driver: a viable option for a light-emitting diode driver for visible light communication. *IEEE Ind Appl Mag*. 2017;23(2):51-61.
3. Li YM, Tong Q, Yang XB, et al. Fixed-frequency adaptive off time controlled buck current regulator with excellent pulse-width modulation and analogue dimming for light-emitting diode driving applications. *IET Power Electron*. 2015;8(11):2229-2236.
4. Hong SS, Lee SH, Cho SH, Roh CW, Han SK. A new cost-effective current-balancing multi-channel LED driver for a large screen LCD backlight units. *J Power Electron*. 2010;10(4):351-356.
5. Cheng CA, Chang CH, Cheng HL, Chung TY, Tseng CH, Tseng KC. A single-stage LED tube lamp driver with input-current shaping for energy-efficient indoor lighting applications. *J Power Electron*. 2016;16(4):1288-1297.
6. Crawford MH. LEDs for solid-state lighting: performance challenges and recent advances. *IEEE J Sel Top Quantum Electron*. 2009;15(4):1028-1040.
7. Wang Y, Alonso JM, Ruan X. A review of LED drivers and related technologies. *IEEE Trans Ind Electron*. 2017;64(7):5754-5765.
8. Li S, Tan SC, Lee CK, Waffenschmidt E, Hui SY(R), Tse CK. (2016)A survey, classification, and critical review of light-emitting diode drivers. *IEEE Trans Power Electron*. 2016;31(2):1503-1516.
9. Kim HC, Choi MC, Kim S, Jeong DK. An AC–DC LED driver with a two-parallel inverted buck topology for reducing the light flicker in lighting applications to low-risk levels. *IEEE Trans Power Electron*. 2017;32(5):3879-3891.
10. Qiu Y, Wang L, Wang H, Liu YF, Sen PC. Bipolar ripple cancellation method to achieve single-stage electrolytic-capacitor-less high-power LED driver. *IEEE J Emerg Sel Top Power Electron*. 2015;3(3):698-713.
11. Wang JM, Wu ST, Yen SC, Lin JY. A simple control scheme for a single stage flyback LED driver. *Int J Circuit Theory Appl*. 2015;43(12):1879-1898.
12. Wang Y, Huang J, Wang W, Xu D. A single-stage single-switch LED driver based on class-E converter. *IEEE Trans Ind Appl*. 2016;52(3):2618-2626.
13. Moon S, Koo GB, Moon GW. Dimming-feedback control method for TRIAC dimmable LED drivers. *IEEE Trans Ind Electron*. 2015;62(2):960-965.
14. Cheng CA, Chung TY. A single-stage LED streetlight driver with PFC and digital PWM dimming capability. *Int J Circuit Theory Appl*. 2016;44(11):1942-1958.
15. Pollock A, Pollock H, Pollock C. High efficiency LED power supply. *IEEE J Emerg Sel Top Power Electron*. 2015;3(3):617-623.
16. Hwu KI, Jiang WZ, Hsiao CW. (2016)Dimmable LED driver based on twin-bus converter and differential-mode transformer. *J Disp Technol*. 2016;12(10):1122-1129.
17. Hwu KI, Jiang WZ, Chen WH. Automatic current-sharing extendable two-channel LED driver with non-pulsating input current and zero dc flux. *Int J Circuit Theory Appl*. 2018;46(8):1462-1484.
18. Liu J, Sun W, Zeng J. Precise current sharing control for multi-channel LED driver based on switch-controlled capacitor. *IET Power Electron*. 2017;10(3):357-367.

19. Qu X, Wong SC, Tse CK. An improved LCLC current-source-output multistring LED driver with capacitive current balancing. *IEEE Trans Power Electron*. 2015;30(10):5783-5791.
20. Chen X, Huang D, Li Q, Lee FC. Multichannel LED driver with CLL resonant converter. *IEEE J Emerg Sel Top Power Electron*. 2015;3(3):589-598.
21. Ramanjaneya Reddy U, Narasimharaju BL. A cost-effective zero-voltage switching dual-output LED driver. *IEEE Trans Power Electron*. 2017;32(12):7941-7953.
22. Borekci S, Acar NC, Kircay A. LED dimming technique without frequency and pulse width modulations. *Int J Circuit Theory Appl*. 2018;46(11):2028-2037.
23. Alonso JM, Perdigao MS, Dalla Costa MA, Martinez G, Osorio R. Analysis and experiments on a single-inductor half-bridge LED driver with magnetic control. *IEEE Trans Power Electron*. 2017;32(12):9179-9190.
24. Qu X, Wong SC, Tse CK. Noncascading structure for electronic ballast design for multiple LED lamps with independent brightness control. *IEEE Trans Power Electron*. 2010;25(2):331-340.
25. Hwu KI, Jiang WZ. Nonisolated two-phase interleaved LED driver with capacitive current sharing. *IEEE Trans Power Electron*. 2018;33(3):2295-2306.
26. Luo Q, Zhi S, Zou C, Zhao B, Zhou L. Analysis and design of a multi-channel constant current light-emitting diode driver based on high-frequency AC bus. *IET Power Electron*. 2013;6(9):1803-1811.
27. Burdio JM, Canales F, Barbosa PM, Lee FC. Comparison study of fixed-frequency control strategies for ZVS DC/DC series resonant converters. IEEE Annual Power Electronics Specialists Conference 2001:427–432.
28. Bęczkowski S, Munk-Nielsen S. LED spectral and power characteristics under hybrid PWM/AM dimming strategy. IEEE Energy Conversion Congress and Exposition Conference 2010:731–735.
29. Chiu HJ, Lo YK, Chen JT, Cheng SJ, Lin CY, Mou SC. A high-efficiency dimmable LED driver for low-power lighting applications. *IEEE Trans Ind Electron*. 2010;57(2):735-743.
30. Moo CS, Chen YJ, Yang WC. An efficient driver for dimmable LED lighting. *IEEE Trans Power Electron*. 2012;27(11):4613-4618.
31. Lun WK, Loo KH, Tan SC, Lai YM, Tse CK. Bilevel current driving technique for LEDs. *IEEE Trans Power Electron*. 2009;24(12):2920-2932.
32. Chang YH, Chen YJ, Chuang YC, Moo CS. Driving circuit for high-brightness LED lamps. International Power Electronics Conference – ECCE 2010:403–407.
33. Rodrigues WA, Morais LMF, Donoso-Garcia PF, Cortizo PC, Seleme SI. Comparative analysis of power LEDs dimming methods, *37th Annual Conference of the IEEE Industrial Electronics Society* IECON 2011:2907–2912.

How to cite this article: Ch KR, Porpandiselvi S, Vishwanathan N. A three-leg resonant converter for two output LED lighting application with independent control. *Int J Circ Theor Appl*. 2019;47:1173–1187. https://doi.org/10.1002/cta.2632